INVESTIGATION OF GOLD NANOPARTICLE MODIFICATION ON SCREEN PRINTED GOLD ELECTRODE BY ELECTROCHEMICAL IMPEDANCE SPECTROSCOPY

Yücel KOÇ[1], Huseyin AVCI[2*]

[1]Department of Chemical Engineering, Eskisehir Osmangazi University, Eskisehir, Turkey
e-posta : yclkoc@gmail.com, ORCID No : https://orcid.org/0000-0002-8301-5595
[2]Department of Metallurgical and Materials Engineering, Eskişehir Osmangazi University, Eşkisehir, Turkey
e-posta : havci@ogu.edu.tr, ORCID No : https://orcid.org/0000-0002-2475-1963

Keywords	Abstract
Screen printed electrode *Gold nanoparticle* *Electrodeposition* *Impedance spectroscopy*	*Recently increasing attention has been paid to the development of highly sensitive and selective electrochemical sensors for accurate and cost-effective detection in various fields. In this study, gold nanoparticles (AuNPs) were electro-deposited onto screen printed gold electrode (SPGE) surfaces at different times to determine the optimum modification conditions. Determining the optimum modification for the SPGE surface, AuNP modification under −0.3 V potential with 2 mM HAuCl$_4$ (in 0.5 M H$_2$SO$_4$) solution were investigated. In this case, for the optimum AuNP modification, electrochemical impedance spectroscopy (EIS) analysis was performed at the following deposition times: 30, 60, 90, 120, and 150 s. As a result of modeling the Nyquist graph obtained in the range of 10 kHz to 0.1 Hz with the EIS analysis based on the equivalent circuit model, the outcomes for each modification time were analyzed. After the modification with AuNPs, scanning electron microscope (SEM) images of the SPGE surfaces were discussed. As a result, the optimum deposition time was determined as 90 s by the analysis. In this study, an electrochemical investigation was carried out with a detailed perspective for the modification of AuNPs on the SPGE surface. In addition, the importance of optimum nanoparticle modification to obtain a smooth electrode surface has been demonstrated, and it is thought that it can help to the researchers for their studies in the field.*

EKRAN BASKILI ALTIN ELEKTROT ÜZERİNE ALTIN NANOPARTİKÜL MODİFİKASYONUNUN ELEKTROKİMYASAL EMPEDANS SPEKTROSKOPİSİ İLE İNCELENMESİ

Anahtar Kelimeler	Öz
Ekran baskılı elektrot *Altın nanoparçacık* *Elektrobiriktirme* *Empedans spektroskopisi*	*Son zamanlarda, çeşitli alanlarda güvenilir ve uygun maliyetli algılama sistemleri için son derece hassas ve seçici elektrokimyasal sensörlerin geliştirilmesi artan bir ilgi ile devam etmektedir. Bu çalışmada altın nanoparçacıklar (AuNP'ler) perde baskılı altın elektrot (SPGE) yüzeyine farklı zaman aralıklarında elektro-biriktirilerek optimum modifikasyon süresi belirlenmiştir. SPGE yüzeyi için optimum modifikasyon belirlenirken, 0,5 M H$_2$SO$_4$ içerisinde hazırlanmış 2 mM HAuCl$_4$ çözeltisi kullanılarak -0,3 V potansiyel uygulamak suretiyle AuNP modifikasyonu gerçekleştirilmiştir. Bu çalışmada ayrıca optimum AuNP modifikasyonu için elektrokimyasal empedans spektroskopisi (EIS) analizi 30, 60, 90, 120 ve 150 s biriktirme sürelerinde gerçekleştirilmiştir. 0.1 Hz ile 10 kHz frekans aralığında elde edilen Nyquist grafiğinin eşdeğer devre modeli ile modellenmesi ile ayrıntılı EIS analizi yapılmış, ek olarak her bir modifikasyon süresi için sonuçlar irdelenmiştir. AuNP'lerin SPGE yüzeylerine modifikasyonundan sonra, taramalı elektron mikroskobu (SEM) analizi ile SPGE yüzeylerinde meydana gelen değişimler çalışmamızda tartışılmıştır. Sonuç olarak, optimum biriktirme süresi 90 s olarak belirlenmiştir. Bu araştırmada SPGE yüzeyine AuNP'lerin modifikasyonu ayrıntılı elektrokimyasal analizler ile geniş bir perspektifte ele alınmıştır. Ayrıca daha iyi bir elektrot yüzeyi elde etmek için optimum nanopartikül modifikasyonun önemi gösterilmiş ve bunun ilgili olan araştırmacıların çalışmalarına yardımcı olacağı düşünülmektedir.*

* Sorumlu yazar; e-posta : havci@ogu.edu.tr

1. Introduction

Electrochemical sensors based on screen-printed electrodes (SPEs) have risen in popularity due to low cost, ease of use, portability, and structural simplicity. SPEs are devices that contain dual or triple electrode systems created by printing different inks on a ceramic or plastic surface (Apetrei and Apetrei, 2018; Zhang, Jiang, Zhang, Zhang, and Li, 2019). SPEs are widely used due to their many advantages, such as low sample volume requirements, comparatively low cost, flexibility, and good reproducibility, especially in developing electrochemical biosensors (Koç, Morali, Erol and Avci, 2021b; Sanzo et al., 2016; Singh, Jaiswal, Tiwari, Foster and Banks, 2018). These electrodes can be easily integrated into portable analytical and industrial systems which are becoming more common in various fields from food to healthcare and environmental industries (Avci, Güzel, Erol, and Akpek, 2018; Couto, Lima, and Quinaz, 2016; Garbioglu, Demir, Ozel, Avci and Dincer, 2021; Güzel et al., 2021; Ozel et al., 2021; Shaegh et al., 2018; Shin et al., 2016; Shin et al., 2017; Zhang et al., 2017)

The modification of the electrodes with metallic nanoparticles draws attention in the various field. Modifications of SPE with metallic nanoparticles provide enormous benefits in detecting lower amounts of target molecules in analysis by increasing the electrode's sensitivity, selectivity, and verifiability (Zhu, Zhu, and Shu, 2022). Gold nanoparticles (AuNPs) are frequently used materials that can increase the active electrode surface area and are very useful for constructing the desired chemical structure on the surface (Stine, 2019; Taurino et al., 2016). Moreover, the high conductivity and catalytic properties of gold nanoparticles indicate that the nanoparticles are used for the electroanalytical determination of a wide variety of analytes (Merli et al., 2016). AuNPs can also improve the detection signal electron transfer, which can improve the limit of detection for the sensors (Charoenkitamorna, Chailapakulac, and Siangproh, 2015). It is known that after the AuNPs are deposited on the electrode surface, it improves the redox properties at the electrode-solution interface. (Huang, Liao, Molesa, Redinger, and Subramanian, 2003). It is also allowing large surface energy and binding of many biomolecules on the electrode surface. (Zeng, Zhu, Du, and Lin, 2016).

Electrochemical impedance spectroscopy (EIS) has appeared as a useful technique to develop biosensors with various modifications which can overcome the difficulties encountered in this context (Wolff, Harting, Heinrich, Röder, and Krewer, 2018). The EIS method is usually performed by symmetrically stimulating the system with either a current or potential perturbations and measuring the response to this stimulus (Morali, 2020). The EIS can be used to study the response of an electrochemical system with small signal effects. It is a very effective technique for identifying and analyzing any point of the system with investigating electrode/electrolyte interfacial properties (Avci, Anıl, Koc, Moralı, and Erol, 2019; Galeotti, Giammanco, Cina, Cordiner, and Di Carlo, 2015; Koç, Morali, Erol and Avci, 2019; Samie and Arvand, 2020). Lastly, EIS has various benefits like low measuring time, simplicity of assessing sensitivity and selectivity, and ease of integration into point-of-care (POC) systems (Koç et al., 2021b).

Since the modification of SPGE surfaces with AuNPs can contribute the excellent performance for a trace detection of molecules, particles and cells of interest, the aim of our study is to discuss electro-d eposition of AuNPs onto SPGEs surfaces at different times to determine the optimum modification conditions. In addition, surface morphology of the sensing electrode was investigated by scanning electron microscopy (SEM).

2. Materials and Methods

2.1. Chemicals

Gold (III) chloride trihydrate ($HAuCl_4 \cdot 3H_2O$) (49% Au, w/v), and Sulfuric acid (H_2SO_4) (98.08%, w/v) were purchased from Sigma-Aldrich. Potassium hexacyanoferrate (II) trihydrate ($K_4Fe(CN)_6 \cdot 3H_2O$) was received from Kimetsan. Phosphate buffer saline (PBS) (1x) was obtained from Thermoscientific.

2.2. Apparatus

Electrochemical measurements require highly sensitive, accurate and suitable ambient conditions. Electrodeposition and electrochemical impedance measurements were carried out using a Reference 3000 Potentiostat/Galvanostat/ZRA. The tests and data analysis were carried out using the Echem Analyst and PSTrace softwares. Gamry Faraday cage was also used to block the electric field created by environmental noise.

Screen printed gold electrodes (SPGE, 220AT model) were purchased from Dropsens (Oviedo, Spain). SPGE (33 mm x 10 mm x 0.5 mm (length x width x height)) contains a gold working electrode, a gold counter electrode, and a silver reference electrode. The working electrode surface area was 0.1256 cm^2. A Hitachi Regulus 8230 Field Emission Scanning Electron Microscope (FESEM) was used to analyze the exterior morphology of the surface of SPGEs. All of the experimental studies were conducted at room temperature (23 °C±2).

2.3. Methods

Research and publication ethics were complied with in this study. It is stated in this article that no legal/special permission is required. SPGE surfaces have been modified to obtain better and more distinct electrodeposition as follows: first, surface activation was performed with 0.5 M H_2SO_4 (50 µl) solution on the electrode surface to obtain a positive electrode surface under an applied potential of −0.6 V. Then, the electrode surface was washed successively with PBS (1x) and ultrapure water. Following the washing, AuNPs modification was performed by using 2 mM $HAuCl_4$ (in 0.5 M H_2SO_4) (50 µl) solution under an applied potential of −0.3 V at 30 s, 60 s, 90 s, 120 s and 150 s electrodeposition times, and the optimum modification time was determined by EIS analysis. After providing each deposition, the SPGE was analyzed by EIS using 2 mM $K_4[Fe(CN)_6]$ in PBS (1x) (50 µl). After the modification, unbound AuNPs were removed by washing with ultrapure water and ethanol, respectively. Fig. 1. shows a schematic representation of AuNPs modification on the SPGE.
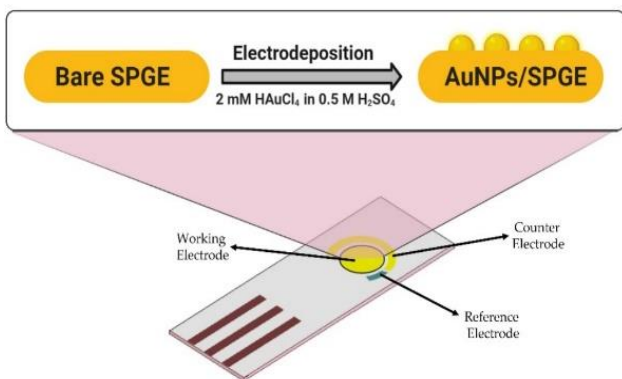

Figure 1. Schematic Illustration of Modification by Using AuNPs on the Electrodeposited SPGE.

3. Result

3.1. Optimum Deposition Time for AuNPs Modified SPGE by EIS Analysis

It is of great importance to determine the optimum modification time for the SPGE surface with AuNPs. While high modification times cause damage to the electrodes, low modification times can prevent AuNPs from being deposited at a sufficient level on the SPGE surfaces.

Nyquist plots of the impedance responses of bare, surface activated, and AuNPs modified SPGEs with different deposition times (30 s, 60 s, 90 s, 120 s, and 150 s) are presented in Fig 2. (a), and suitable equivalent circuit model is shown in Fig 2. (b).
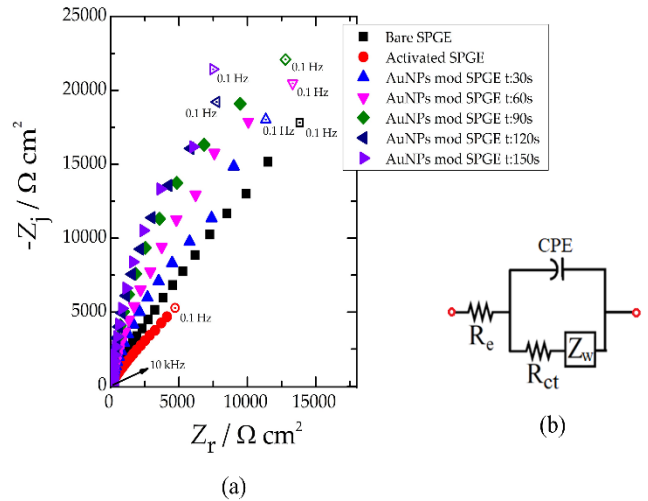

(a)

(b)

Figure 2. (a) Nyquist Plot of Impedance Responses for AuNPs Modified SPGE with Different Deposition Times from 30 s to 150 s in 2 mM $K_4[FE(CN)_6]$ in PBS (1mM). (b) Equivalent Randles Circuit Model for Nyquist Plot.

EIS, based on measuring the current through the cell by applying a periodic AC potential to the system analysis of an electrochemical cell (Lasia, 2002), is a type of transfer function measurement often used in the analysis of the systems (Wang et al., 2021). The frequency-dependent transfer function examines electrochemical systems in detail by measuring the system's response (current, potential) to this perturbation. The impedance, Z, can be expressed as (Wang et al., 2021):

$$Z(\omega) = \frac{\tilde{V}}{\tilde{I}} = \left|\frac{\tilde{V}(\omega)}{\tilde{I}(\omega)}\right| (\cos\phi(\omega) + j\sin\phi(\omega)) = Z_r + j Z_j \qquad (1)$$

The variables $\tilde{V}$ (potential) and $\tilde{I}$ (current) are phasors, time-independent numbers describing the amplitude and phase of a sinusoidal function. ϕ is the phase angle between the input and output signals (Wang et al., 2021). In equation (1), ω expresses the angular frequency, and j is the imaginary complex number which are defined as:

$$\omega = 2\pi f \qquad (2)$$

$$j = \sqrt{-1} \qquad (3)$$

The Randles equivalent circuit model is shown in Fig. 2. (b) was developed to fit the impedance data of the SPE electrochemical system. The corresponding impedance Z in the equivalent Randles circuit model can be expressed as (Orazem and Tribollet, 2008):

$$Z = R_e + \frac{R_{ct} + Z_w}{1 + (j\omega)^\alpha (R_{ct} + Z_w)Q} \qquad (4)$$

Impedance responses were quantified using the mathematical model depicted in Equation 4, which was based on the suitable equivalent Randles circuit model. The Simplex method of the regression analysis algorithm with the Echem Analyst software built in Gamry was used to fit parameters. The values of the parameters along with their confidence intervals are shown in Figure 3, and the corresponding values in integer notation for the obtained results are demonstrated in Table 1.
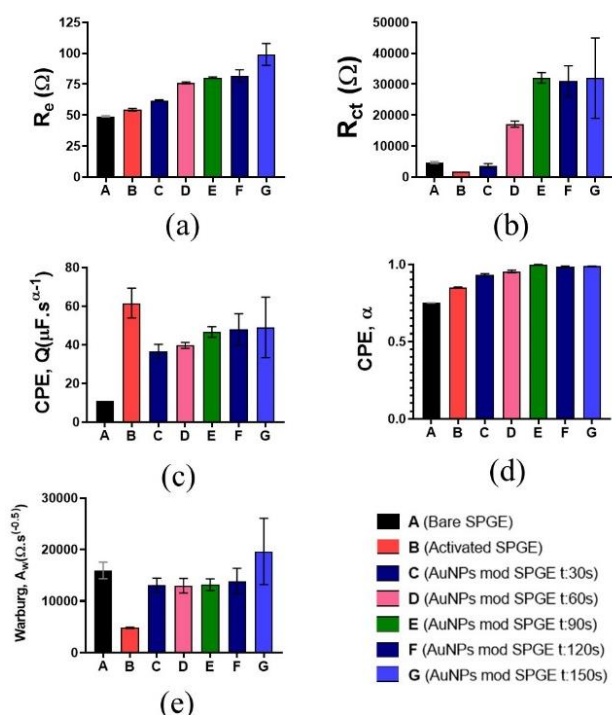

Figure 3. Regression Results with Confidence Intervals for The Equivalent Circuit Model Parameters. (a) Ohmic Resistance, R_e, (b) Charge-Transfer Resistance, R_{ct}, (c) CPE Coefficient, Q, (d) CPE Exponent, α, (e) Warburg Coefficient A_w.

Electrolyte resistance (R_e) or ohmic resistance refers to the resistance of the contact between the electrode/electrolyte interface, which occurs as a result of inhibition of the transfer of ions from the redox solution. The electrolyte resistance is determined by comparing the voltage recorded by the reference electrode as a result of the analysis with the input and output voltages of the system. The interception of the real axis of the Nyquist plot in the high frequency region yielded the electrolyte resistance (R_e) parameter. The electrolyte resistance (ohmic resistance) of a solution is affected by concentration, temperature, ion type, and effective electrode area (Koç, Morali, Erol, and Avci, 2021a). As shown in Fig. 3 (a), although electrolyte solutions, their concentrations, and environmental conditions are the same, their ohmic resistances seem to increase as the deposition time increases due to the modification of AuNPs on the electrode surfaces. The observed increase in ohmic resistance appears to be due to the change in the active area of the electrodes.

Charge transfer resistance (R_{ct}), obtained by the width of the high-frequency capacitive loop, is related to the electrode/electrolyte interface and generally results from the electrochemical reactions taking place on the SPGE surfaces (Wang et al., 2021). The charge transfer resistance is obtained by moving ions in the electrolyte to the electrode and identifying the electrodes surface modification layers. The current flow resulting from charge transfer depends on the concentration of the transferred ions, the potential resulting from the electrochemical reactions, and the products of the reaction. As shown in Fig. 3 (b), it was revealed that the R_{ct} of SPGE was reduced due to surface activation. The R_{ct} value increased linearly as the modification time was increased, and after a 90 s modification with AuNPs, the increase in R_{ct} value disappeared, and the highest value was observed at 90 s followed by a plateau around 120 s and 150 s times. It can be concluded that the error margin of R_{ct} value increased even more in the deposition times after 90 s.

The region between the electrode surface and the surrounding electrolyte is modeled using a constant phase element (CPE), which is one of the electrical circuit elements. CPE is defined as a defective capacitor with these two charge layers at the interface between electrolyte and the rough electrode surface. As shown in Fig. 3 (c), the modification of AuNPs to the SPGE surfaces resulted in an increase in effective capacitance associated with the CPE coefficient Q. Its activated surface caused an increase in the capacitance values. While the capacitance (CPE) was 11.04 µF before the surface activation, it increased to 61.53 µF after the activation. During the activation, the electrode surface is exposed to a negative potential, and as a result, the electrode surface becomes positively charged. The positively charged electrode surface has better electrical conductivity and electron transfer. The higher the capacitance of the electrode before AuNPs modification, the higher its ability to store charges (Borah, Bharali, and Morris, 2017; Iskandar, Abdillah, Stavila, and Aimon, 2018). It was also observed that the capacitance value increased as the deposition time increased. The increase in error of capacitance values was mainly

observed at higher deposition times. CPE exponent α is an indicator of roughness of the electrode surfaces and the current distribution on the surfaces. α is usually between 0.5 and 1. A value close to 1 indicates that the roughness is low, the current is evenly distributed over the surface, and the electrode exhibits a capacitive-like behavior (Jorcin, Orazem, Pebere, and Tribollet, 2006). As shown in Fig. 3 (d), modification of AuNPs on the surfaces of SPGE yields a higher CPE exponent. The higher CPE exponent, the more uniform charge distribution on the electrode. The CPE exponent was analyzed to be the highest at 90 s and remained stable within 120 s and 150 s deposition times.

Warburg impedance refers to the ion diffusion occurring at the electrodes in equivalent circuit modeling. As shown in Fig. 3 (e), the Warburg value decreased after the surface activation and then increased again upon AuNPs modification. It can be seen that greater the deposition time led to higher the error value. The regressed all parameters and their confidence levels of the model are presented in Table 1.

Table 1.

Regression Results of Equivalent Circuit Model Parameters and Their ±σ Confidence Intervals of a Fit of Equation (4) to the Data Represented in Figures 2. (a).

Parameter	R_e (Ω)	R_{ct} (Ω)	Q, (μF s$^{α-1}$)	$α$	A_w, (Ω s$^{-0.5}$)
Bare SPGE	48.96±0.58	4263±293	11.04±0.01	0.751±0.01	15938±1629
Activated SPGE	54.37±1.07	1666.62±5.53	61.53±3.73	0.851±0.03	4812±123
AuNPs mod SPGE t:30s	61.80±0.47	2606.91±703.4	36.64±3.61	0.942±0.07	13089±1360
AuNPs mod SPGE t:60s	76.10±0.76	17087±1307.02	39.65±1.54	0.973±0.09	12987±1413
AuNPs mod SPGE t:90s	83.31±0.57	32045±2687.22	46.62±2.68	0.998±0.11	13171±1113
AuNPs mod SPGE t:120s	83.65±6.01	29950±4990	47.93±8.11	0.984±0.54	13879±2462
AuNPs mod SPGE t:150s	99.08±5.83	31950±12990	48.93±15.68	0.987±0.22	19629±6432

3.2. SEM Analysis

SEM images of the bare and AuNPs modified SPGE are presented in Fig. 4.

When the SEM image of the working electrode region of the bare and modified SPGEs was examined, it was observed that the bare electrode had a porous structure with occasional indentations and protrusions. After the porous SPGE electrode surface was coated with AuNP, the porosity of the surface was reduced. Therefore, AuNPs modified SPGE process seems to be successful. Also, the significant increase in CPE exponent α value in Fig. 3. (d) also proves this situation. As the electrodeposition time increased, darkening occurred in the real image of the electrodes due to oxidation. In the analysis of the EIS results in Fig. 3, it is seen that the errors value increase as the deposition time increases.

In addition, Wan et al. reported that blackening occurred at the reference electrode when AuNP modification was made on SPGE (Wan et al., 2015). Therefore, the results of electrochemical examination using EIS and morphological analyses results using SEM are compatible to describe data.
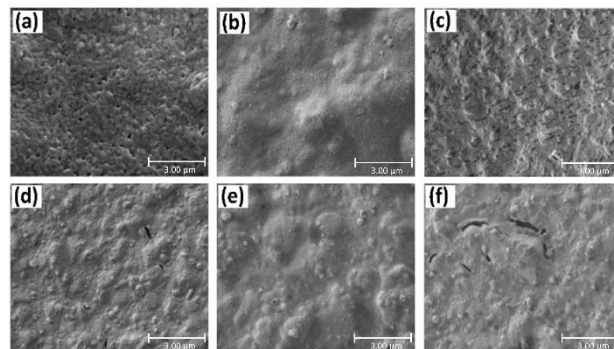

Figure 4. SEM Images of AuNPs on Working Electrode of SPGE at Different Deposition Times; (a) Bare SPGE at t:0s, (b) t:30s, (c) t:60s, (d) t:90s, (e) t:120s, (f) t:150s.

(scale bar: 3 μm)

4. Conclusion

The performance of commercial SPGEs with AuNPs modification was investigated using a systematic experimental design. In this study, AuNPs electrodeposition was performed on the SPGE surface and optimum deposition time was determined by the electrochemical impedance spectroscopy (EIS) method. EIS analysis was performed at deposition times of 30, 60, 90, 120, and up to 150 s. The impedance of the resulting circuit model for each modification period was analyzed by modeling the Nyquist plot obtained by EIS analysis with the equivalent circuit model. As a result of the examination, it was seen that the 90 s modification time had the highest R_{ct} and α values. It was also observed that the error values in the results of the equivalent circuit model parameter increased after 90 seconds of the accumulation time. After the modification, AuNPs deposited on the SPGE surface were also evaluated by scanning electron microscopy (SEM) in which the SPGE surface was not deformed at the optimum 90 s modification time. However, the deformation occurred on the electrode surface at higher modification times. Therefore, the optimum acceptable deposition time for modification of AuNPs on SPGEs was determined to be 90 s. This approach can be used as a simple and sensitive method for other alternative modifications in the literature for the determination of target analytes in the real complex samples.

Author Contributions

Yücel Koç designed the experiment, analyzed the electrochemical data, conceptualization, writing – original draft, drew the figures, and discussed the results. Huseyin Avci conceptualized the paper, supervision, project administration, discussed the results, and reviewed the manuscript

Conflict of Interest

There is no conflict of interest.

References

Apetrei, I. M., & Apetrei, C. (2018). A modified nanostructured graphene-gold nanoparticle carbon screen-printed electrode for the sensitive voltammetric detection of rutin. *Measurement* 114, 37–43. doi: https://doi.org/10.1016/j.measurement.2017.09.020

Avci, H., Anıl H., Koc, Y., Moralı, U., & Erol, S. (2019). Developing biosensors for food safety analysis. *4th International Congress on Biosensors*, Çanakkale, Turkey.

Avci, H., Güzel, F. D., Erol, S., & Akpek, A. (2018). Recent advances in organ-on-a-chip technologies and future challenges: a review. *Turkish Journal of Chemistry*, 42(3), 587-610. doi: https://doi.org/10.3906/kim-1611-35

Borah, D., Bharali, D. K., & Morris, M. A. (2017). Lignocellulosic-based activated carbon prepared by a chemical impregnation method as electrode materials for double layer capacitor. *Advances in Chemical Engineering and Science*, 7(02), 175. doi: https://doi.org/10.4236/aces.2017.72013

Charoenkitamorn, K., Chailapakul, O., & Siangproh, W. (2015). Development of gold nanoparticles modified screen-printed carbon electrode for the analysis of thiram, disulfiram and their derivative in food using ultra-high performance liquid chromatography. *Talanta,* 132: 416-423. doi: https://doi.org/10.1016/j.talanta.2014.09.020

Couto, R. A. S., Lima, J. L. F. C., & Quinaz, M. B., (2016). Recent developments, characteristics and potential applications of screen-printed electrodes in pharmaceutical and biological analysis. *Talanta*, 146, 801-814. doi: https://doi.org/10.1016/j.talanta.2015.06.011

Galeotti, M., Giammanco, C., Cinà, L., Cordiner, S., & Di Carlo, A., (2015). Synthetic methods for the evaluation of the State of Health (SOH) of nickel-metal hydride (NiMH) batteries. *Energ. Convers. Manage*, 92,1-9. doi: https://doi.org/10.1016/j.enconman.2014.12.040

Garbioglu, D., Demir, N., Ozel, C., Avci, H., & Dincer, M. (2021). Determination of therapeutic agents efficiencies of microsatellite instability high colon cancer cells in post-metastatic liver biochip modeling. *The FASEB Journal*, 35(9), e21834. doi: https://doi.org/10.1096/fj.202100333R

Güzel, F. D., Ghorbanpoor, H., Dizaji, A. N., Akcakoca, I., Ozturk, Y., Kocagoz, T., Corrigan, D., & Avci, H. (2021). Label-free molecular detection of antibiotic susceptibility for Mycobacterium smegmatis using a low cost electrode format. *Biotechnology and Applied Biochemistry*, 68(6), 1159-1166. doi: https://doi.org/10.1002/bab.2037

Huang, D., Liao, F., Molesa, S., Redinger, D., & Subramanian, V. (2003). Plastic-compatible low resistance printable gold nanoparticle conductors for flexible electronics. *Journal of the electrochemical society*, 150(7), G412. doi: https://doi.org/10.1149/1.1582466

Iskandar, F., Abdillah, O. B., Stavila, E., & Aimon, A. H., (2018). The influence of copper addition on the electrical conductivity and charge transfer resistance of reduced graphene oxide (rGO). *New Journal of Chemistry*, 42(19), 16362-16371. doi: https://doi.org/10.1039/C8NJ03614D

Jorcin, J.-B., Orazem, M. E., Pébère, N., & Tribollet, B. (2006). CPE analysis by local electrochemical impedance spectroscopy. *Electrochimica Acta*, 51(8-9), 1473–1479. doi: https://doi.org/10.1016/j.electacta.2005.02.128

Koc, Y., Moralı, U., Erol, S., & Avci, H. (2019). Investigation of immobilization process of screen printed carbon electrode for an advanced biosensor

a detailed characterization. *IV. International Scientific and Vocational Studies Congress - Engineering*, Ankara, Turkey.

Koç, Y., Moralı, U., Erol, S., & Avci, H. (2021a). Investigation of electrochemical behavior of potassium ferricyanide/ferrocyanide redox probes on screen printed carbon electrode through cyclic voltammetry and electrochemical impedance spectroscopy. *Turkish Journal of Chemistry*, 45(6). doi: http://doi.org/10.3906/kim-2105-55

Koç, Y., Moralı, U., Erol, S., & Avci, H. (2021b). Electrochemical investigation of gold based screen printed electrodes: an application for a seafood toxin detection. *Electroanalysis*, 33(4), 1033-1048. doi: https://doi.org/10.1002/elan.202060433

Lasia, A. (2002). Applications of electrochemical impedance spectroscopy to hydrogen adsorption, evolution and absorption into metals. *In Modern aspects of electrochemistry* (pp. 1-49). Springer, Boston, MA. doi: https://doi.org/10.1007/0-306-47604-5_1

Merli, D., Ferrari, C., Cabrini, E., Dacarro, G., Pallavicini, P., & Profumo, A. (2016). A gold nanoparticle chemically modified gold electrode for the determination of surfactants. *RSC advances*, 6(108), 106500-106507. doi: https://doi.org/10.1039/C6RA22223D

Morali, U. (2020). Synergistic influence of charge conditions on electrochemical impedance response of LiNiMnCoO2|C coin cells - Complementary statistical analysis. *Journal of Energy Storage*, 32, 101809. doi: https://doi.org/10.1016/j.est.2020.101809

Orazem, M. E., & Tribollet, B. (2008). Electrochemical impedance spectroscopy. *New Jersey*, 383-389.

Özel, C., Koç, Y., Topal, A., Ebrahimi, A., Şengel, T., Ghorbanpoor, H., Doğan Guzel, F., Uysal, O., Eker Sarıboyacı, A. & Avcı, H. (2021). Investigation of 3d culture of human adipose tissue-derived mesenchymal stem cells in a microfluidic platform. *Eskişehir Technical University Journal of Science and Technology A-Applied Sciences and Engineering, 22(8th ULPAS-Special Issue 2021),* 85-97. doi: https://doi.org/10.18038/estubtda.983881

Samie, H. A., & Arvand, M., (2020). Label-free electrochemical aptasensor for progesterone detection in biological fluids, *Bioelectrochemistry*, 133, 107489. doi: https://doi.org/10.1016/j.bioelechem.2020.107489

Sanzo, G., Taurino, I., Antiochia, R., Gorton, L., Favero, G., Mazzei, F., Micheli, & Carrara, S. (2016). Bubble electrodeposition of gold porous nanocorals for the enzymatic and non-enzymatic detection of glucose. *Bioelectrochemistry*, 112, 125-131. doi: https://doi.org/10.1016/j.bioelechem.2016.02.012

Shaegh, S. A. M., Pourmand, A., Nabavinia, M., Avci, H., Tamayol, A., Mostafalu, P., & Zhang, Y. S. (2018). Rapid prototyping of whole-thermoplastic microfluidics with built-in microvalves using laser ablation and thermal fusion bonding. *Sensors and Actuators B: Chemical*, 255, 100-109. doi: https://doi.org/10.1016/j.snb.2017.07.138

Shin, S. R., Kilic, T., Zhang, Y. S., Avci, H., Hu, N., Kim, D., ... & Khademhosseini, A. (2017). Label-Free and regenerative electrochemical microfluidic biosensors for continual monitoring of cell secretomes. *Advanced Science*, 4(5), 1600522. doi: https://doi.org/10.1002/advs.201600522

Shin, S. R., Zhang, Y. S., Kim, D. J., Manbohi, A., Avci, H., Silvestri, A., & Khademhosseini, A. (2016). Aptamer-based microfluidic electrochemical biosensor for monitoring cell-secreted trace cardiac biomarkers. *Analytical chemistry*, 88(20), 10019-10027. doi: https://doi.org/10.1021/acs.analchem.6b0202

Singh, M., Jaiswal, N., Tiwari, I., Foster, C. W., & Banks, C. E. (2018). A reduced graphene oxide-cyclodextrin-platinum nanocomposite modified screen printed electrode for the detection of cysteine. *J. Electroanal. Chem.* 829, 230–240. doi: https://doi.org/10.1016/j.jelechem.2018.09.018

Stine, K. J. (2019). Biosensor Applications of Electrodeposited Nanostructures. *Applied Sciences*, 9(4),797. doi: https://doi.org/10.3390/app9040797

Taurino, I., Sanzò, G., Antiochia, R., Tortolini, C., Mazzei, F., Favero, G., Michelii, & Carrara, S. (2016). Recent

advances in third generation biosensors based on Au and Pt nanostructured electrodes. *TrAC Trends in Analytical Chemistry*, 79, 151-159. doi: https://doi.org/10.1016/j.trac.2016.01.020

Wan, H., Sun, Q., Li, H., Sun, F., Hu, N., & Wang, P. (2015). Screen-printed gold electrode with gold nanoparticles modification for simultaneous electrochemical determination of lead and copper. *Sensors and Actuators B: Chemical*, 209, 336-342. doi: https://doi.org/10.1016/j.snb.2014.11.127

Wang, S., Zhang, J., Gharbi, O., Vivier, V., Gao, M., & Orazem M. (2021). Electrochemical impedance spectroscopy. *Nat Rev Methods Primers,* 1, 41. doi: https://doi.org/10.1038/s43586-021-00039-w

Wolff, N., Harting, N., Heinrich, M., Röder, F., & Krewer, U. (2018). Nonlinear frequency response analysis on lithium-ion batteries: a model-based assessment. *Electrochimica Acta*, 260, 614-622. doi: https://doi.org/10.1016/j.electacta.2017.12.097

Zeng, Y., Zhu, Z., Du, D., & Lin, Y. (2016). Nanomaterial-based electrochemical biosensors for food safety. *Journal of Electroanalytical Chemistry*, 781, 147-154. doi: https://doi.org/10.1016/j.jelechem.2016.10.030

Zhang, Y. S., Aleman, J., Shin, S. R., Kilic, T., Kim, D., Mousavi Shaegh, S. A., & Khademhosseini, A. (2017). Multisensor-integrated organs-on-chips platform for automated and continual in situ monitoring of organoid behaviors. *Proceedings of the National Academy of Sciences*, 114(12), E2293-E2302. doi: https://doi.org/10.1073/pnas.161290611

Zhang, Y., Jiang, X., Zhang, J., Zhang, H., & Li, Y. (2019). Simultaneous voltammetric determination of acetaminophen and isoniazid using MXene modified screen-printed electrode. *Biosensors and Bioelectronics*, 130, 315-321. doi: https://doi.org/10.1016/j.bios.2019.01.043

Zhu, W., Zhu, A., & Shu, Y. (2022). GNP/CNT nanocomposite coated screen-printed electrode for point-of-care testing of dopamine in human serum. *Progress in Organic Coatings*, 170, 106983. doi: https://doi.org/10.1016/j.porgcoat.2022.106983